Available online at www.sciencedirect.com
SCIENCE DIRECT®
Journal of Physiology - Paris 98 (2004) 19–34
Journal of Physiology Paris
www.elsevier.com/locate/jphysparis

Multiplication and stimulus invariance in a looming-sensitive neuron

Fabrizio Gabbiani [a,*], Holger G. Krapp [b], Nicholas Hatsopoulos [c], Chun-Hui Mo [d], Christof Koch [d], Gilles Laurent [d]

[a] Division of Neuroscience, Baylor College of Medicine, One Baylor Plaza, Houston, TX 77030, USA
[b] Department of Zoology, University of Cambridge, Downing Street, Cambridge, CB2 3EJ, UK
[c] Department of Organismal Biology and Anatomy, University of Chicago, 1027 East 57th Street, Chicago, IL 60637, USA
[d] Division of Biology, California Institute of Technology, Pasadena, CA 91125, USA

Abstract

Multiplicative operations and invariance of neuronal responses are thought to play important roles in the processing of neural information in many sensory systems. Yet the biophysical mechanisms that underlie both multiplication and invariance of neuronal responses in vivo, either at the single cell or at the network level, remain to a large extent unknown. Recent work on an identified neuron in the locust visual system (the LGMD neuron) that responds well to objects looming on a collision course towards the animal suggests that this cell represents a good model to investigate the biophysical basis of multiplication and invariance at the single neuron level. Experimental and theoretical results are consistent with multiplication being implemented by subtraction of two logarithmic terms followed by exponentiation via active membrane conductances, according to $a \times 1/b = \exp(\log(a) - \log(b))$. Invariance appears to be in part due to non-linear integration of synaptic inputs within the dendritic tree of this neuron.

Keywords: Looming; LGMD; DCMD; Multiplication; Invariance; Single neuron computation

1. Introduction

The cellular and dendritic mechanisms involved in sensory information processing within single neurons and among networks of cells have been intensely investigated in the past few years [34,78]. Still very little is known, however, about how biophysical properties of nerve cells implement neuronal computations in vivo. Two such computations thought to be of fundamental importance are the multiplication of independent signals and the generation of invariant responses.

A classical example of a multiplicative computation is the extraction of directional motion information from a two-dimensional image, described in insects by the correlation model of Reichardt and Hassenstein [27] (Fig. 1A). This model is formally equivalent to the motion-energy model in primates [1], including humans, and relies on a multiplication operation between neighboring light sampling stations on the animal's retina. The biophysical implementation of these so-called "elementary movement detectors" (EMDs) that are thought to multiply adjacent retinal inputs still remains unsolved to this day, in spite of more than 40 years of work [8]. Other examples of neural computations that are thought to involve multiplicative interactions include the generation of directionally selective responses in rabbit retinal ganglion cells [6] (Fig. 1B). Similar mechanisms might underlie directional selectivity in cortical neurons [3,39] or govern the sensitivity of midbrain auditory neurons [48]. Gain fields, i.e., the modulation of sensory receptive fields according to the direction of gaze in parietal neurons [2], also appears to be of multiplicative nature (Fig. 1C), as is the modulation of receptive field properties by attention in areas V4 and MT of the monkey visual cortex [40,81]. In none of these examples has the biophysical implementation been fully explained, although models have been proposed and recent experimental advances have clarified the biophysical mechanisms that might be at work [13,16,18].

Invariance of neuronal responses is a widespread aspect of sensory processing that characterizes the extraction of features independent of their context [12].

* Corresponding author.
E-mail address: gabbiani@bcm.tmc.edu (F. Gabbiani).

0928-4257/$ - see front matter © 2004 Elsevier Ltd. All rights reserved.
doi:10.1016/j.jphysparis.2004.03.001

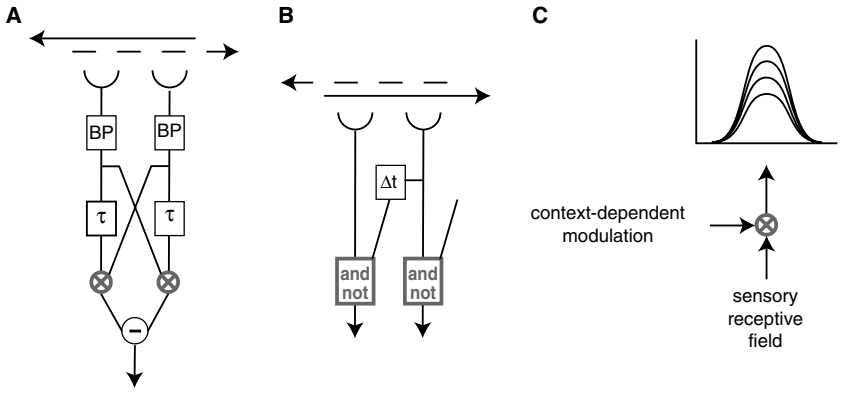

Fig. 1. Multiplications have been implicated in several neural computations. (A) The elementary movement detector model effectively implements a correlation operation between adjacent photoreceptor inputs multiplied together after a fixed delay (τ) in one of the input channels. Subtraction of two mirror symmetrical units yields a fully directional output. This model accurately describes the detection of motion, both at the behavioral and neuronal level, in several insect species. (B) Directional selectivity of motion detection in retinal ganglion cells has been described by a different, delayed inhibitory veto mechanism originally proposed by Barlow and Levick. In A and B the solid and dashed arrows indicate the preferred and anti-preferred directions of the motion detectors, respectively. (C) The receptive fields of neurons in several cortical areas of the monkey visual cortex have been shown to scale up or down in a multiplicative manner by varying a second contextual variable, for example attention to the stimulus.

Invariant visual responses have for example been described in the inferotemporal cortex of macaque monkeys, where many neurons respond to specific objects with an increase in mean firing rate that is largely independent of object size or position in the visual field [62,71]. Such invariance properties could play a role in the processing of visual and other sensory information leading to stimulus categorization [69]. It is presently unknown whether the mechanisms that underlie this specificity are due to single cell or network mechanisms. Another example is the contrast invariance of orientation tuning in V1 cortical neurons [17]. In this instance, recent experimental and theoretical work has clarified candidate biophysical mechanisms that may contribute to this property [4,26,43].

In the locust visual system, both multiplication and invariance appear to be at work in the processing of looming stimuli [19,22,28]. Multiplication arises at the level of an identified neuron in the computation of an angular threshold that could be used for collision avoidance with looming objects. Invariance of this angular threshold computation to various characteris-

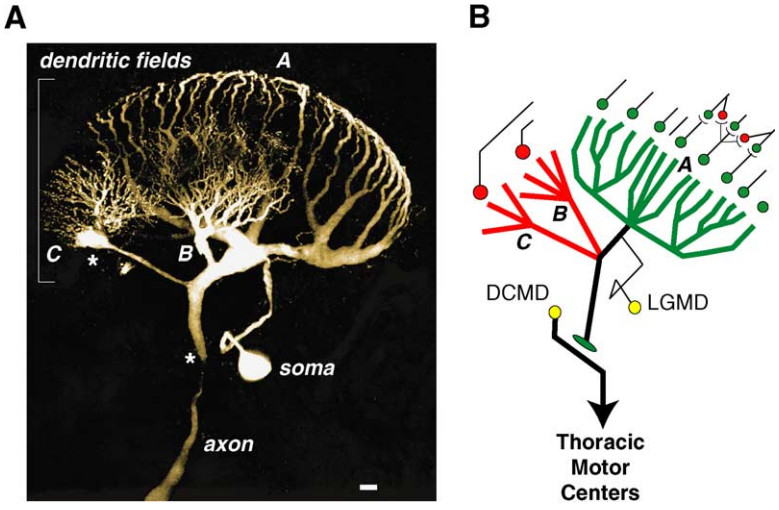

Fig. 2. Anatomy of an escape circuit in the locust. (A) The LGMD neuron's dendritic tree consists of three distinct subfields (A–C). Subfield A receives motion-sensitive excitatory inputs while subfields B and C receive phasic inhibition related to object size. The soma lies outside of the electrical signal propagation path and spikes are generated at the point where the axon is thinnest. (B) Schematic illustration of the neuronal inputs received by the LGMD. Postsynaptic inhibitory regions of the LGMD are illustrated in red and excitatory ones in green. Green and red dots schematize inhibitory and excitatory synapses respectively. Yellow dots indicate cell bodies. Note the lateral inhibitory network thought to be mediated by inhibitory (red) synapses between excitatory presynaptic afferents to dendritic field A. The LGMD synapses in the protocerebrum onto the DCMD neuron that transmits spikes in 1–1 manner to thoracic motor centers. Adapted from [20].

tics of looming objects is an important aspect of neuronal responses. In the following sections, we first review experimental and theoretical analyses of this model system and then compare the results to those obtained in some of the other systems briefly described above.

2. Computation of an angular threshold by a looming-sensitive neuron

The lobula giant movement detector (LGMD) is an identified neuron in the third visual neuropil of the locust optic lobe (lobula) that responds vigorously to objects approaching on a collision course with the animal [57,70] (Fig. 2A). The firing rate of the LGMD can be monitored by recording extracellularly the action potentials of its post-synaptic target neuron in the contralateral nerve cord, the descending contralateral movement detector (DCMD; Fig. 2B). The synaptic contact between the LGMD and the DCMD is formed by a mixed chemical and electrical synapse that is so powerful as to transmit LGMD's spikes in a 1–1 manner to the DCMD with a typical delay of 1–2 ms [32,47]. Thus, under visual stimulation, each spike in the DCMD is caused by a spike in the LGMD and vice-versa. The responses of the LGMD/DCMD to looming stimuli have been investigated by simulating the approach of black squares or disks on a bright background along a trajectory perpendicular to the animal's eye (Fig. 3A). The LGMD responds throughout object approach with a firing rate that first increases, then peaks and finally decays towards the end of approach [19,28] (Fig. 3C). If we denote by l the object half-size and by v its approach velocity, the angular size subtended at the retina by the object during approach is given by

$$\theta(t) = 2\tan^{-1}(l/vt). \quad (1)$$

In this equation the variable t denotes time to collision of the object with the animal, conventionally chosen to be negative prior to collision. According to this convention, the velocity v is negative (<0) for an approaching object. In the following we will denote by speed the absolute value of the velocity ($|v| > 0$). In locusts as in most insects, eyes are located on either side of the head and their region of binocular overlap is small compared with the total solid angle covered by the eye (e.g., in the horizontal plane, binocular overlap extends for <20° compared to almost 180° of visual sampling per eye) [31,73]. Because the receptive field of the LGMD is monocular and each eye views largely independent portions of visual space, $\theta(t)$ fully describes the time course of retinal stimulation by the approaching object. It follows from Eq. (1) that both the angular size $\theta(t)$ and the angular velocity of expansion ($\dot{\theta}(t)$) are non-linear functions of time during looming approach (Fig. 3B). Another observation that can be made from Eq. (1) is that the temporal dynamics of $\theta(t)$ and $\dot{\theta}(t)$ depends only on the ratio, $l/|v|$, of the object's half-size, l, to its approach speed, $|v|$. The experimental values of $l/|v|$ used in the experiments described below ranged from 5 to 50 ms,

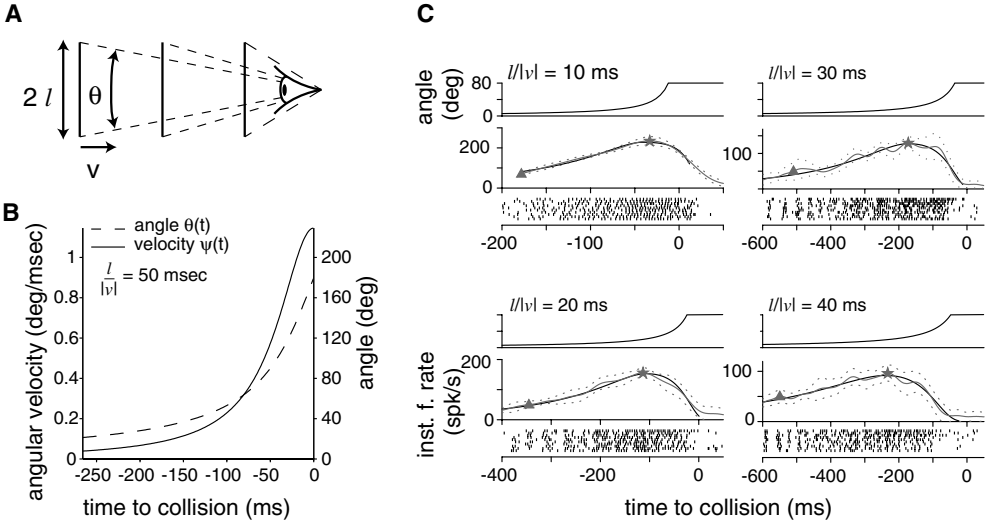

Fig. 3. Extracellular recordings from the LGMD/DCMD neurons in response to looming stimuli. (A) Solid objects (typically black squares on a bright background) are presented on a straight collision course with the animal. The approach speed, $|v|$, is constant and l denotes the object half-size. The angular size, θ is computed from l and v by trigonometry (Eq. (1)). (B) Both the angle subtended by the object and the angular expansion velocity are non-linear functions of time during the approach. (C) Responses elicited by looming squares approaching at different values of the parameter $l/|v|$ (10, 20, 30 and 40 ms, respectively). In each case the time course of the angular size subtended by the object at the retina is illustrated on top. The middle traces are the instantaneous firing rate estimates (grey lines ± sd) and model fits (black; see Section 5) Bottom rasters are spikes elicited in 10 different presentation of the stimulus. Stars: peak instantaneous firing rate. Triangles: arbitrary threshold firing rate of 50 spk/s (see Section 6). Adapted from [19,20].

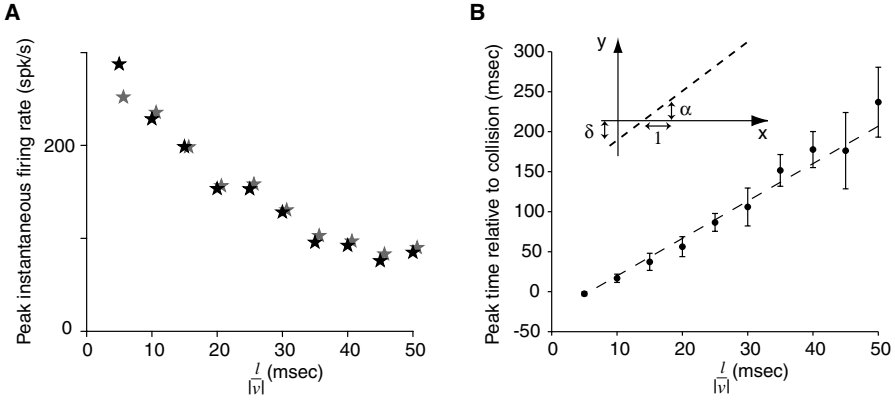

Fig. 4. Dependence of peak firing rate and peak firing time relative to collision on $l/|v|$. (A) The peak firing rate is plotted as a function of $l/|v|$ for the neuron illustrated in Fig. 3C. Grey stars are experimental values and black stars are fits with the model described in Section 5. (B) Peak firing time (mean ± standard deviation) is plotted as a function of $l/|v|$ in a different neuron. The inset illustrates the definition of the linear fit parameters α (slope of the linear fit) and δ (intercept with the y-axis). Adapted from [19,20].

corresponding to approaches lasting between 0.5 and 6 s for objects sizes ranging between 12 and 28 cm at approach speeds between 2 and 10 m/s (see [19, Table 1]).

As the looming parameter $l/|v|$ is varied over one order of magnitude (5–50 ms), the overall time-course of the LGMD's firing rate remains largely unchanged, consisting of an increase followed by a peak and a subsequent decrease (Fig. 3C; [19]). However, several systematic changes occur as $l/|v|$ is varied. First, responses are typically brisker for small or fast approaching objects, leading to higher peak firing rates (Fig. 4A). Second, the timing of the peak consistently shifts towards collision as the parameter $l/|v|$ decreases (Figs. 3C and 4B). Plotting peak firing time relative to collision as a function of $l/|v|$ reveals a relation that is very close to linear (Fig. 4B) and that can therefore be described by fitting a straight line to the data and computing its intercept with the y-axis, δ and its slope, α (Fig. 4B, inset). It can be shown from Eq. (1) that such a linear relation is equivalent to the angular size subtended by the object being a fixed constant δ ms prior to the peak, independent of the stimulation parameter $l/|v|$ ([19, Appendix 1]). This angular threshold size can be computed from the slope of the linear fit, $\theta_{\text{thres}} = 2\tan^{-1} 1/\alpha$, and is typically in the range of 15–35° [19]. Thus, LGMD's peak firing time acts as an angular threshold detector, signaling with a delay of δ ms (between 15 and 35 ms) the time at which an object reaches a fixed angular size on the retina (Fig. 5).

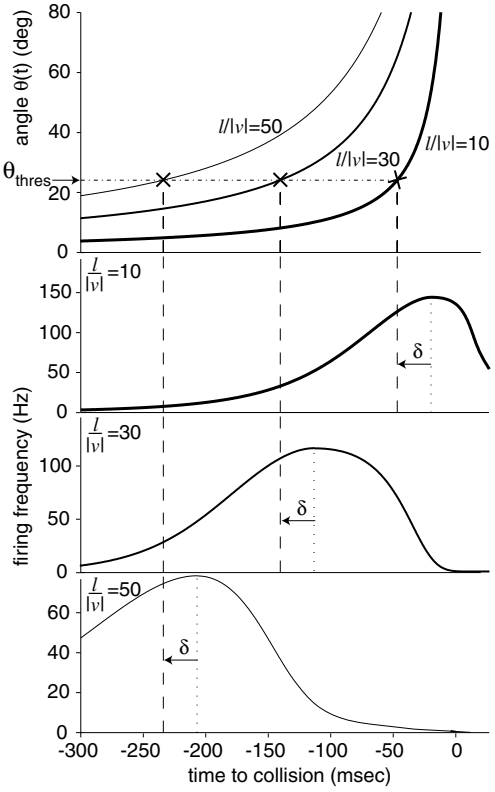

Fig. 5. Peak firing rate signals that an angular threshold has been exceed δ ms earlier. The time-course of angular size is depicted in the top panel for three approaches at different values of $l/|v|$. The mean angular size subtended by the object δ ms prior to the peak for each approach is indicated by the crosses. The corresponding time-course of the instantaneous firing rate is illustrated in the bottom three panels (with each panel corresponding to a different value of $l/|v|$). The position of the peak firing rate is indicated by the dotted lines and the moment in time preceding the peak by δ ms by the dashed lines. Note that the value of θ_{thres} is independent of $l/|v|$, as may be read from the ordinate of θ_{thres} on the top panel. Adapted from [19].

3. Invariance of LGMD's responses to looming stimulus parameters

If angular threshold is used to trigger escape responses or collision avoidance maneuvers, one should expect it to be encoded independent of the particular properties of looming stimuli or conditions of stimulus presentation. We tested this hypothesis by systematically varying sev-

eral experimental parameters and monitoring their effect on the linear relation between $l/|v|$ and LGMD's peak firing time. The linear relation between $l/|v|$ and peak firing time was independent of the luminance and contrast of the looming objects as well as of the overall body temperature [19], which is expected to increase significantly during flight, for instance [84]. The linear relation between $l/|v|$ and peak firing time was also independent of variations in the shape of the approaching object, its texture and its approach angle within most of the horizontal plane, as illustrated in Fig. 6 [22]. Invariance to luminance and contrast is likely to be achieved by local, peripheral gain control mechanisms at the level of the lamina or medulla, as described in several insect species [37,38]. Temperature constancy is presumably obtained through homeostatic mechanisms controlling the activation dynamics of ionic membrane channels [42,87]. In contrast, invariance to shape, texture or approach direction is expected to be implemented within the dendritic tree of the LGMD itself, since local retinotopic inputs are first integrated at the level of the dendrites of the cell (see Section 4).

The responses of the LGMD to looming stimuli can be described in terms of a model based on a multiplicative combination of angular velocity and size described in more detail in next section [19,22,28]. Simulations of a two-dimensional version of this model, based on linear summation of excitatory and inhibitory inputs and a point neuron structure for the LGMD reproduce the linear relationship between $l/|v|$ and peak firing time for solid objects approaching on a trajectory perpendicular to the eye (Fig. 7A; [22]). The model fails, however, to predict invariance to changes in object texture or approach angle (Fig. 7B–D). This suggests

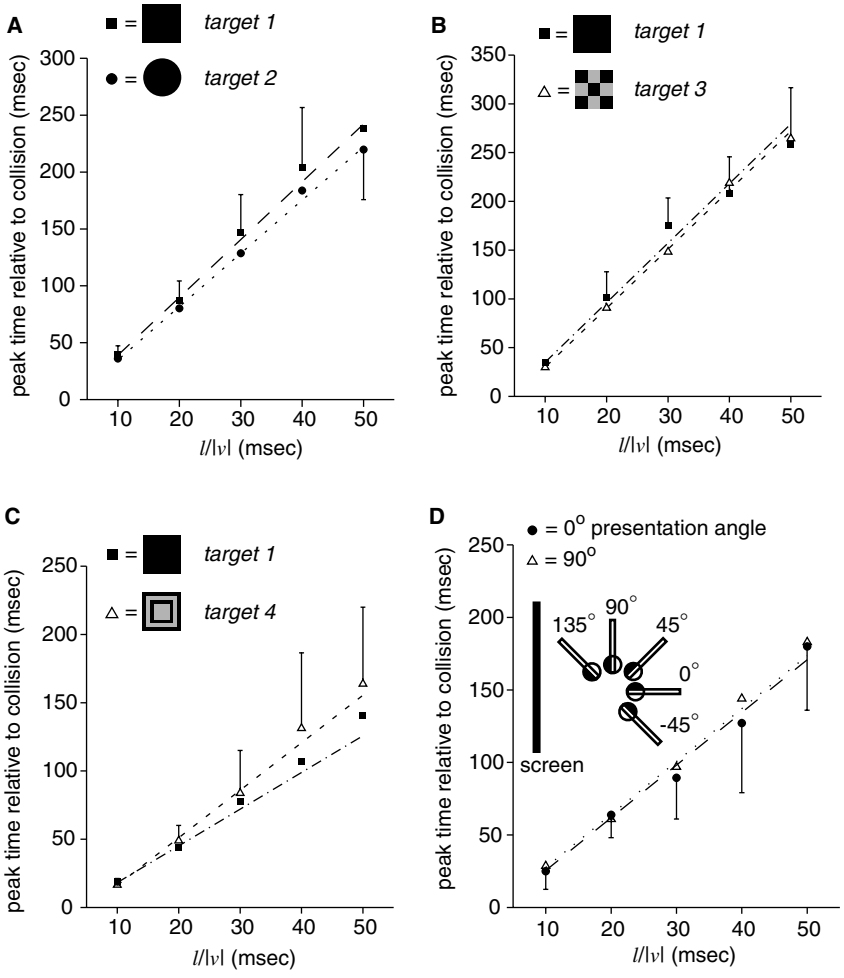

Fig. 6. Invariance of angular threshold computation to looming stimulus parameters. Looming stimulis with different characteristics were presented to the same animal and the timing of the peak firing rate was monitored as a function of $l/|v|$. (A) Peak firing time as a function of $l/|v|$ remained unchanged for solid squares or discs. (B) and (C) Peak firing time as a function of $l/|v|$ remained unchanged for different object textures (checker board pattern and concentric squares, respectively). (D) Peak firing time as a function of $l/|v|$ was independent of presentation angle over a large range of values. Data is compared for two presentation angles (objects looming straight in front of the animal or perpendicular to the long body axis). The schematic inset shows the range of angles tested for the orientation of the animal's eye relative to the screen. The stimulated eye is shown in black. Adapted from [22].

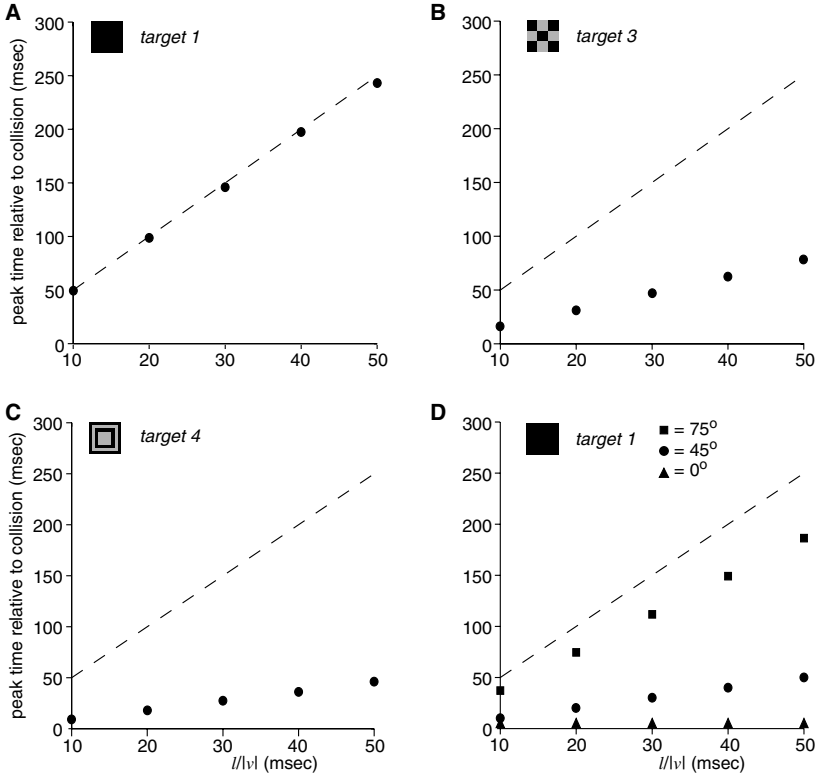

Fig. 7. Peak firing time as a function $l/|v|$ obtained from the responses of a 2-D model of the LGMD based on linear summation of motion-sensitive excitation and size-dependent inhibition in a point-like neuron. (A) The model peak firing time as a function of $l/|v|$ (black dots) reproduces experimental data (dashed line) for straight on approach of a solid black square. (B)–(D) The model fails to reproduce the peak firing time invariance observed for textured objects or different approach angles (see Fig. 6), suggesting that at least one of the two assumptions used to construct the model (linear summation and point-like dendritic structure) is incorrect. Adapted from [22].

that the integration of synaptic inputs within the LGMD is non-linear or that its dendritic tree structure and conductances play an important role in filtering incoming excitation and inhibition. Preliminary results (Supplementary material of Ref. [20]) suggest that at least the first hypothesis is true: in terms of the resulting firing rate, the summation of excitatory inputs within the LGMD's dendritic tree is highly non-linear. This point is illustrated in Fig. 8A. Animals were placed in a semi-circular apparatus consisting of six independent stimulation stations [35]. Each station contained a small (7.8°) black disc on a white background that could be moved along a circular trajectory (10°) at various speeds and positions in the receptive field of the LGMD/DCMD. The peak firing rate and total number of spikes elicited by these moving targets were monitored during motion of individual targets or simultaneous activation of several targets at various positions in the visual field (Fig. 8A, inset). When compared with the linear prediction obtained from summation of individual responses, both the peak firing rate and the number of spikes elicited by simultaneous target activation where highly non-linear (Fig. 8A), consistent with sublinear summation of excitatory inputs within the dendritic tree of the LGMD.

4. Anatomical and physiological characterization of the LGMD's inputs

The LGMD dendritic tree arborizes in three subfields within the lobula (Fig. 2A) that receive distinct inputs [47]. The properties of these inputs have been partially characterized anatomically and physiologically. In a frontal projection, such as the one illustrated in the microphotograph of Fig. 9A (see also Fig. 2A), dendritic subfield A has the appearance of a large fan of dendrites radiating from a sturdy main branch situated on the posterior side of the optic lobe. The distal tips of the dendrites in subfield A form a crescent and appear strongly stained because they are close to the anterior surface while the fan and main branch are progressively more faint due to their deeper location, close to the posterior surface of the optic lobe. Reconstructions based on confocal microscopic sections reveal clearly the 3-dimensional structure of the fan: its dendritic branches run in depth along the distal edge of the lobula where they intersect afferent fibers projecting from the medulla. Two distinct types of medullary cells have been reported to project towards the lobula, with one axon of each cell type per visual column [77]. Both have been described anatomically as T-cells, that is, the arrangement between

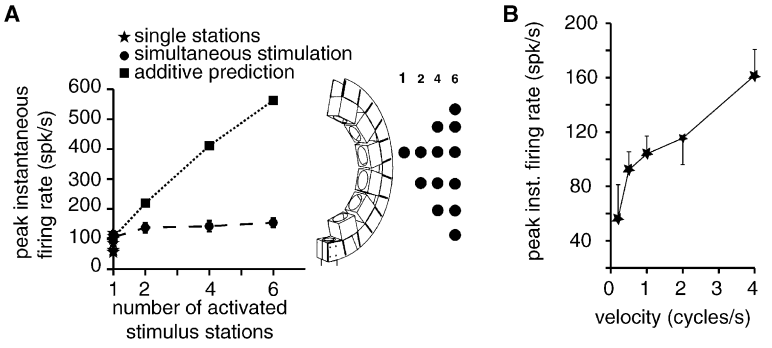

Fig. 8. Firing characteristics of the LGMD/DCMD to local motion stimuli. (A) Peak instantaneous firing rate (black dots connected by the dashed line) in response to local stimulation with 1, 2, 4 or 6 discs moving simultaneously at various positions in the LGMD's receptive field (as illustrated in the inset). Stars are peak firing rates elicited by each disc activated independently at the same six positions. Squares are predictions obtained by summing linearly the responses to each individual station. (B) Peak firing rate as a function of dot speed (1 cycle = 360°) for a single stimulus activated close to the center of the eye.

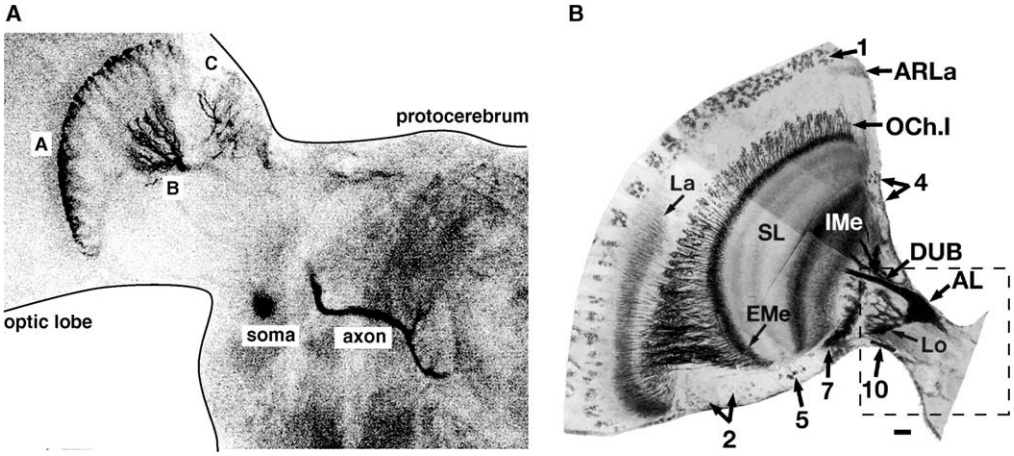

Fig. 9. LGMD anatomy in relation to optic lobe anatomy. (A) Microphotograph of a Lucifer yellow stained LGMD neuron taken from the anterior side of the optic lobe and protocerebrum. The most strongly stained portions of the cell (tip of the dendrites in subfield A and subfields B and C) are close to the anterior surface while the fan fades towards its main branch. The main branch is located close to the posterior surface of the optic lobe (see also Fig. 2A). (B) NADPH-diaphorase stain of the optic lobe revealing some of its characteristic features. Note the strong staining of the dorsal uncrossed bundle (DUB) which projects onto dendritic field C of the LGMD in the anterior lobula (AL). The cell bodies of the corresponding neurons are indicated by arrow 7 in the second optic chiasm. The dashed rectangle indicates the approximate position and size of the microphotograph in panel A. *Abbreviations*: La, lamina; OCh.I, first optic chiasm; EMe, exterior medulla; IMe, interior medulla; SL, serpentine layer; Lo, lobula. *Scale bar*: 50 μm. The anatomical properties of cell types 1, 2, 4, 5, 7 and 10 are described in Ref. [15]. Panel B adapted with permission from [15]. Copyright 1996 the Company of Biologists, Ltd.

their dendritic-axonal axis and the fiber leading to the cell body is T-shaped (see Fig. 1d of Ref. [74]). One type of T-cell extends to the outer medulla while the second type is confined below the serpentine layer to the inner medulla (Fig. 9B). It is presently unknown whether only one or both of these fiber types make synaptic contacts onto the LGMD. This is reminiscent of the anatomy of the fly visual system, where T4 and T5 cells arborizing in the inner medulla and lobula, respectively, are thought to be presynaptic to lobula plate tangential cells (LPTCs) [7,75]. The axons of these LGMD afferents have been reported to range in diameter from 15 to 25 μm in the medulla, and to decrease to 5–7 μm as they enter the lobula [56]. Immunocytochemical evidence suggests that they contain acetylcholine and that postsynaptic receptors onto the LGMD are nicotinic, thus mediating excitatory inputs to the fan [56]. The anatomical arrangement of these projection fibers implies that synaptic contacts onto dendritic field A are organized in a retinotopic manner. A similar arrangement is seen in fly LPTCs and retinotopy has been confirmed physiologically by correlating local calcium concentration increases with local motion stimuli in LPTCs visual receptive fields [14]. Such direct proof is still lacking in the case of the LGMD.

The afferent input to dendritic field A is thought to mediate the spiking responses of the LGMD to small stimuli moving in its receptive field (Fig. 8). These

responses are elicited irrespective of the direction of object motion and depend on object speed (Fig. 8B). Additional physiological evidence supports the notion that motion dependent excitation impinges on dendritic subfield A and suggests the type of information that could be conveyed by the afferent fibers. First, the excitatory response of the LGMD to small moving objects habituates rapidly upon repeated presentation and this habituation is specific to the stimulated region, i.e., retinotopic [46]. Because dendritic subfields B and C appear to receive non-retinotopic inputs [77], this rules them out as candidate recipients of retinotopic, motion-sensitive excitation. In fact, additional experiments summarized below strongly suggest that subfields B and C receive inhibitory inputs. Local habituation transfers from ON to OFF stimuli and vice-versa [46]; it is therefore assumed that the input to subfield A is mediated by ON/OFF fibers responding to contrast changes independent of their polarity (dark-to-light and vice-versa). Consistent with this view, the LGMD responds in a similar manner to small ON or OFF static stimuli flashed in its receptive field [66]. Since electrical stimulation of afferent fibers in the second optic chiasm elicits habituation of EPSPs in the LGMD, it is thought that the site of habituation is located at the synapses between afferent fibers and the fan itself [46]. There is little evidence for post-synaptic habituation, although adaptation mechanisms similar to those observed in fly LPTCs cannot be ruled out at present [36]. An important aspect of the motion-dependent excitatory input received by the LGMD is that it is subject to a lateral inhibitory network, first evidenced by O'Shea and Rowell (Figs. 2B and 10) [45]. The anatomical location of this lateral inhibitory network has not yet been unambiguously determined and two neuropils, the medulla and lobula have been proposed as candidate locations [59,67]. The most recent hypothesis is based on anatomical data: the excitatory afferents to dendritic field A of the LGMD make reciprocal cholinergic synapses between themselves [59]; similar synapses have also been reported in the fly among afferents presynaptic to LPTCs [75,76]. It has been suggested that these synapses are muscarinic and could mediate lateral inhibition via G-protein mediated receptors [59]. Pharmacological block of muscarinic transmission in the lobula could help to confirm this hypothesis [21,82]. Local excitatory interactions between adjacent excitatory afferents to the fan have not been described thus far. It is nevertheless possible that motion dependent excitation to the LGMD conveys non-directional information by averaging over different directions inputs such as those mediated by a half-correlation detector scheme [89]. In particular, a half-correlation motion detector will respond to static ON or OFF stimuli in a manner that is similar to pure ON/OFF fibers as described above. Additional experiments are needed to characterize more precisely the dependence of the excitatory input on moving vs. stationary stimuli.

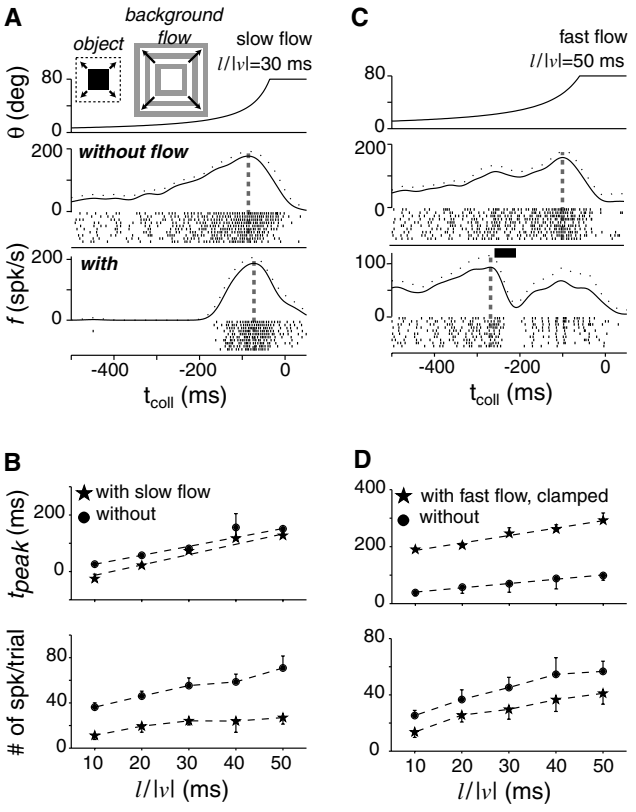

Fig. 10. Responses of the LGMD/DCMD to looming stimuli with or without a background flow activating either lateral (A) and (B) or feedforward inhibition (C) and (D). (A) Top panel shows the time course of the looming stimulus on the retina. Middle panel is instantaneous firing rate (mean ± sd) and spike rasters (10 trials) in response to the looming stimulus alone. Bottom panel is instantaneous firing rate and spike rasters in response to the looming stimulus and a grey/white background of stripes slowly moving outwards. Vertical dashed grey lines indicate peak firing time. (B) Peak firing rate time (top) and number of spikes elicited per trial (bottom) in the two conditions depicted in A (mean ± sd). (C) Same as A, but the background stimulus appears abruptly and transiently for 50 ms (black horizontal bar). (D) Same as in B for the experiment depicted in C. Adapted from [20].

Current evidence is consistent with dendritic subfields B and C receiving feedforward inhibitory inputs (Fig. 2B). This inhibition was first evidenced in experiments of O'Shea and Rowell, demonstrating that large, transient ON/OFF stimuli effectively curtailed the excitation caused by small translating stimuli in the LGMD's receptive field [45]. Feedforward inhibition is observed in intracellular recordings of the LGMD's membrane potential to consist of IPSPs causing a weak hyperpolarization (typically 5–10 mV) with respect to rest (Fig. 11A and D). Although precise conductance measurements have not been performed, these results are consistent with shunting of membrane conductance being an important factor in controlling excitation. The IPSPs mediated by phasic ON and OFF transients differ in

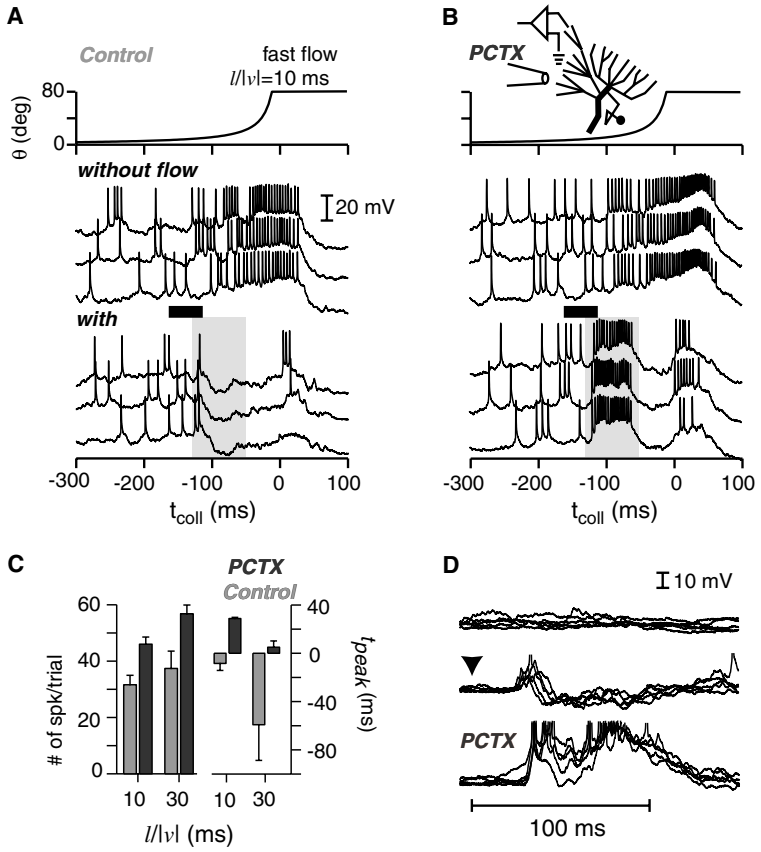

Fig. 11. Effect of local picrotoxin injection in the lobula on responses of the LGMD to looming stimuli. (A) Top panel is time-course of the looming stimulus on the retina. Top three intracellular traces (dendritic recording from the LGMD neuron) are responses to this stimulus and bottom three traces are responses to the same stimulus and the fast background flow (black horizontal bar; see also Fig. 8C). Note the IPSPs highlighted by the light grey box (bottom three traces). (B) Same as A after picrotoxin injection. The responses are prolonged and a strong EPSP replaces the IPSP observed in control conditions (light grey box). (C) Number of spikes per trial (left) and peak firing time (right) before and after picrotoxin injection (dark grey and light grey, respectively). (D) Effect of presenting the fast background flow stimulus alone (in the absence of looming stimuli). Arrowhead marks the onset of stimulation. Note the IPSP in control condition (middle traces) and the large EPSP after picrotoxin application. Top traces are responses to blank screen. Adapted from [20].

several aspects, suggesting that different pathways are involved [67]. The neurons providing input to dendritic subfield C have been characterized anatomically: their cell bodies are located at the level of the second optic chiasm (arrow 7 in Fig. 9B) and the extent of their dendritic arborizations in the medulla is consistent with receptive fields 8×12 deg in size [67]. The axons of these neurons converge to form a bundle of approximately 500 fibers 2 μm thick called the dorsal uncrossed bundle (DUB [25]; Fig. 9B). Sectioning the DUB specifically abolishes inhibition to phasic OFF transients while leaving the inhibition to ON transients unaffected [67]. These results are consistent with subfields C and B providing phasic OFF and ON inhibition, respectively. Inputs to subfield B have not yet been characterized anatomically; they are believed to be mediated by a second uncrossed (non-retinotopic) bundle of fibers, the median uncrossed bundle [25,77]. Local application of the GABA blocker picrotoxin in the lobula inactivates feedforward inhibition (Fig. 11; [20]), consistent with inhibition being mediated by $GABA_A$ synapses at the level of the LGMD [52,86].

5. Biophysical implementation of the angular threshold computation

How could the inputs described in the previous section combine to generate the characteristic firing rate of the LGMD during looming object approach? This question was first investigated at the theoretical level by looking for combinations of angular velocity and angular size that can account for the observed shape of the LGMD/DCMD firing rate during looming. Linear combinations of angular velocity and size (such as $[\dot{\theta}(t) - \alpha\theta(t)]$ or $[\dot{\theta}(t) - \exp(\alpha\theta(t))]$) could not reproduce experimental data while the multiplicative combination $[\dot{\theta}(t)\exp(-\alpha\theta(t))]$ was successful over a limited range of $l/|v|$ values (between 5 and 25 ms; [28]). The same multiplicative model could be extended over the whole

range of $l/|v|$ values (5–50 ms) by passing the output of the multiplicative combination of angular velocity and size through a static power-law non-linearity (x^n, with two distinct n values for the rise and decay phase of the response; for details, see refs. [19,20]). Because the LGMD receives both feedforward excitatory inputs that are motion- and velocity-dependent and feedforward inhibitory inputs that are size-dependent, this suggests that it might act as a biophysical device multiplying postsynaptically its two inputs related to expansion velocity and size of the object during approach.

This hypothesis was tested experimentally by assessing the relative role played by lateral and feedforward inhibition in controlling motion-dependent excitation during looming. Because lateral inhibition is presynaptic to the LGMD on the excitatory motion-dependent pathway, it could play an important role in controlling excitation as an object grows on the retina [54,55]. We designed stimuli that selectively activated lateral and feedforward inhibition and presented them concurrently to looming stimuli (Fig. 10). Both activation of lateral and feed-forward inhibition reduced the excitation caused by an approaching object, however, the time window during which they were effective was markedly different. Activation of lateral inhibition was able to control excitation early during the trial (Fig. 10A and B). As soon as the looming object exceeded about 23° on the retina, lateral inhibition was completely ineffective and consequently the timing of the LGMD's peak firing rate and the linear relation between $l/|v|$ and peak firing time were only slightly affected by its activation. In contrast, activation of feed-forward inhibition was highly effective at reducing excitation, even during periods of high LGMD activity (Fig. 10C and D). These experimental results suggest that as a looming object grows on the retina, feedforward inhibition progressively outweighs lateral inhibition. We further investigated the role played by feed-forward inhibition during looming object approach by local application of the GABA antagonist picrotoxin in the lobula (Fig. 11). Because lateral inhibition is presumably mediated in the lobula by muscarinic acetylcholine receptors between excitatory afferent fibers presynaptic to the LGMD (see Section 4; [59]), this pharmacological manipulation selectively inactivated feedforward inhibition.

After blocking feedforward inhibition by picrotoxin injection, the responses of the LGMD to looming stimuli were greatly prolonged in duration (Fig. 11A–C) with an increased number of spikes and peak firing rates almost twice as high as in control trials (Fig. 11C). The angle subtended by the object when the firing rate in picrotoxin trials started to significantly exceed the firing rate in control trials [20] was then calculated. On average, this angle amounted to 23.3° and was therefore closely related to the angle at which lateral inhibition starts to lose its efficacy in controlling excitation. These results suggest that feedforward inhibition is able to effectively counteract excitation over more than 2/3 of the angular values taken by the stimulus during simulated object approach (from 23.3° to 80°) and that it therefore plays a predominant role in controlling feedforward excitation. Thus, the multiplicative operation observed at the level of the LGMD's firing rate is most likely due to interaction between postsynaptic feedforward excitation and inhibition within the LGMD itself rather than occurring presynaptically.

If the multiplicative combination between angular velocity and angular size is implemented within the LGMD, one possible biophysical mechanism would be to subtract these two components in logarithmic coordinates, followed by exponentiation, i.e., $a \times 1/b = \exp(\log(a) - \log(b))$, a trick commonly used in analog integrated circuits [41]. The exponentiation operation might be implemented at the level of the spike initiation zone by sodium channels that convert membrane voltage to firing rate. To test this hypothesis, the membrane potential in response to looming stimuli close to the spike initiation zone was recorded and its conversion into firing rate studied [20]. The first point considered was whether sodium channels contribute in any other way than postulated by the logarithmic-exponential model to the transformation of membrane potential. This point was addressed by recording looming responses before and after application of the sodium channel blocker TTX close to the spike initiation zone. Topical application of TTX abolished the spiking activity of the LGMD, leaving peak membrane depolarization to looming stimuli unaffected (Fig. 12A,B). In contrast, application of TTX in the second optic chiasm onto presynaptic afferent fibers to the LGMD completely abolished its responses. Fig. 12B plots the membrane potential recorded during looming before and after TTX application in the same neuron (top and bottom panels, respectively). Prior to TTX application, the subthreshold response was extracted from the spiking response by median filtering (orange traces in Fig. 12A and B). A comparison of the membrane potential time-course in these two conditions revealed a considerable shift of the responses towards later times after TTX application. This was quantified as illustrated in Fig. 12C by plotting the membrane potential time-course (averaged over several trials) in both conditions and calculating an average delay over the rising phase of the response during looming. The delay between subthreshold membrane potential time-courses in control and TTX conditions exceeded 150 ms on average [20]. Thus, sodium conductances appear to phase-advance the response of the LGMD during looming, in addition to their role in converting membrane voltage to firing rate. Next, the transformation of membrane voltage into firing rate was studied by plotting one variable against the other across $l/|v|$ trials. Fig. 12D illustrates the

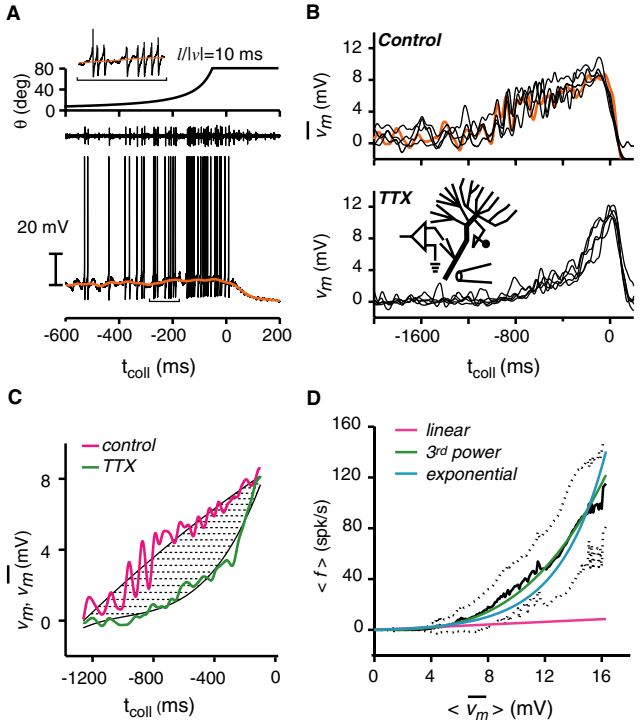

Fig. 12. Transformation between membrane voltage and instantaneous firing rate at the spike initiation zone. (A) Top panel shows the time-course of the looming stimulus at the retina, middle trace is extracellular recording from the DCMD and bottom trace is intracellular recording from the LGMD neuron. Orange line is the subthreshold membrane potential envelope obtained by median filtering. Inset: bracketed portion of the intracellular membrane potential time-course expanded three times. (B) Time course of the membrane potential envelope in the absence (top panel) and presence (bottom) of TTX injected locally to block sodium conductances (inset). Orange trace is same recording as in A. Note the temporal shift of the membrane potential depolarization towards later times after TTX application. (C) Magenta and green traces are mean membrane potential obtained by averaging single trials of B in control and TTX conditions, respectively. The average temporal shift was obtained by taking the mean time difference between these traces (mean length of the black horizontal lines). (D) Plot of the instantaneous firing rate as a function of the mean, median filtered membrane potential during looming object approach (mean ± sd, solid and dotted black lines, respectively). Magenta, green and cyan lines are fits to linear, third power and exponential functions, respectively. Adapted from [20].

average value of the firing rate during looming calculated over successive 5 ms bins and plotted against the corresponding average value of the subthreshold membrane potential (extracted by median filtering). Fits of this instantaneous firing rate as a function of membrane potential were well described by a third power static non-linearity (Fig. 12D, green line), close but not identical to an exponential (Fig. 12D, cyan line), in 7 out of 10 LGMD neurons analyzed [20]. This result suggests that a transformation close to an exponentiation is implemented, at least in part, at the level of the spike initiation zone by sodium sensitive conductances.

6. Behavioral significance of the angular threshold computation

The DCMD axon is among the largest in the thoracic connectives (15 μm in diameter; [44]). Its action potentials will therefore be the first visually triggered signals to reach thoracic motor centers during the approach of a threatening danger. Because the DCMD neuron synapses onto various interneurons and motor neurons involved in flight steering and jump initiation, its has long been thought to be involved in the generation of escape or collision avoidance behaviors [10,50]. Early long-term recordings using chronically implanted electrodes from behaving animals have however failed to find a clear correlation between the DCMD activity and behavior [64]. Its involvement in the generation of escape responses has therefore sometimes been questioned (see Section 9.5.2.1 of [9]). Establishing a causal connection between the LGMD/DCMD firing rate and motor programs eliciting escape or collision avoidance responses has been further complicated by several factors. First the activity of the LGMD/DCMD can be variable in experimental preparations and will sometimes habituate rapidly upon repeated stimulus presentation [65]. This contrasts with observations in minimally restrained, freely behaving animals [63]. While the characteristic timing of the LGMD/DCMD peak activity in response to looming stimuli is robust to habituation (see, e.g., Ref. [19, Fig. 3 and corresponding discussion]), it can be significantly altered in extreme cases [53]. Second, the pattern of synaptic connections made by the DCMD onto target neurons has been shown to be variable in inbred locust colonies [49]. This is probably due to a lack of selective pressure since variability is almost non-existent in wild animals [68]. Third, the pattern of DCMD activity is altered during ongoing motor programs [29,90] and by neuromodulatory inputs [5], suggesting that it is highly context dependent. Finally, around 20 other identified visual neurons have been described in the lobula responding to looming stimuli and that are likely to send visual information to thoracic motor centers as well [24]. Presently, the characteristic of their responses and their relation to the DCMD activity remain unknown.

In the nucleus rotundus of the pigeon visual system, Sun and Frost have described one class of neurons that has very similar response properties to those seen in the LGMD/DCMD and that is therefore able to signal angular threshold size (Fig. 13; [79]). These authors have also reported the existence of two additional classes of cells that signal an angular velocity threshold and time-to-contact, respectively. Thus, several computations might be performed in parallel on visual inputs by neurons involved in generating escape or collision avoidance responses.

Many of the observations described above were made before the sensitivity of the LGMD/DCMD to looming

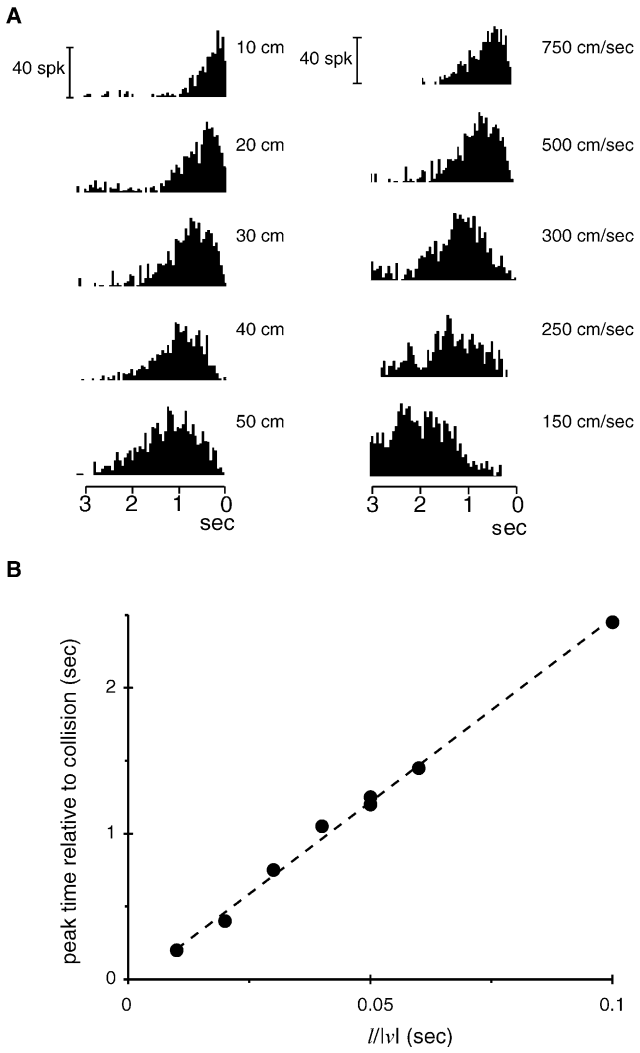

Fig. 13. Responses of a class of pigeon nucleus rotundus neurons to looming objects are similar to those of the LGMD neuron. (A) Histograms of spikes as a function of time to collision obtained in response to looming objects varying in size (left) and approach speed (right). (B) When peak firing time is plotted as a function of the stimulation parameter $l/|v|$ one obtains a linear relation equivalent to the one observed in the LGMD. Adapted with permission from [79]. Copyright 1998 Nature Publishing Group.

stimuli was firmly established [51,57,70] and before specific hypotheses on the information encoded by its firing rate were proposed [19,28]. Because peak DCMD firing rate encodes an angular threshold size, this could be the image-based variable used to trigger escape responses in locusts. It has indeed been found more recently in immobilized animals that a leg flexion can be elicited in response to a looming stimulus [28]. This leg flexion is presumably a preparation for jumping and follows by a fixed delay (~20 ms) the DCMD's peak firing time. Tethered flying locusts confronted with approaching objects have been shown, depending on stimulus characteristics, to either initiate flight steering behaviors or to extend their legs as if preparing for landing. In these experiments, angular threshold size has also been shown to be the variable most closely correlated with the initiation of these collision avoidance maneuvers [60,61]. The timing of the responses suggests that a smaller angular threshold size (10°) than the one typically encoded in the LGMD's peak firing rate is used. Such angular threshold sizes are well encoded by a threshold in DCMD firing rate of 50 spk/s. This may be seen by plotting the time at which the firing rate exceeds 50 spk/s as a function $l/|v|$: the relation is linear with a slope corresponding to an angle of ~10° (see Figs. 1 and 3C of [20]). A similar linear relation is observed between the time of steering reactions and $l/|v|$ at the behavioral level (see Fig. 11 of [23]). Besides the DCMD activity, information from additional neurons is likely to be used to generate directional steering in frontal approaches, because the sensitivity of the LGMD/DCMD in the frontal part of the visual field is low [22,23]. Taken together, these results demonstrate a correlation between the occurrence of an angular threshold size, the LGMD/DCMD activity and escape behaviors, although they do not yet establish a causal relation between these variables.

7. Implementing expansive static non-linearities with membrane conductances and noise

The experiments described in Section 5 raise the question of how the LGMD neuron integrates excitatory and inhibitory synaptic inputs and subsequently converts the resulting membrane potential into a firing rate. This issue will probably best be addressed by a combination of experimental techniques to characterize the time-course of excitatory and inhibitory postsynaptic currents and potentials in response to looming stimuli and by biophysical compartmental modeling techniques. Some experimental results obtained recently in other preparations shed light on this issue.

First, shunting inhibition has been classically described to mediate non-linear, multiplicative interactions between excitatory and inhibitory subthreshold membrane potentials [80], particularly when it is located on the path of excitation to the spike initiation zone [33], as is the case for the inhibition mediated by dendritic subfields B and C of the LGMD (Fig. 2). However, more recent work has revealed that the effect of shunting inhibition can be more complex in the suprathreshold regime of a spiking neuron. In cases where synaptic noise plays a relatively minor role, shunting inhibition has a subtractive effect on firing rates [30], whereas when synaptic noise is important, its net effect is divisive [13]. These results have been obtained in steady-state conditions and their relevance to highly dynamic situations such as those encountered during the presentation of looming stimuli remains to be investigated.

Synaptic noise has also been shown to play an important role in the transformation of membrane potential into firing rate in a group of simple and complex cells of cat primary visual cortex [4]. In these neurons, membrane voltage is converted into firing rate according to a power law and synaptic noise can explain how such static non-linearities arise from linear threshold models (Fig. 14A; [11]). More recent theoretical work has shown that such power law transformations are necessary to explain orientation-tuning invariance of the firing rate to changes in contrast in terms of the orientation invariant membrane voltage tuning observed experimentally [26,43]. The mapping of membrane voltage to firing rate according to an expansive non-linear transformation is likely to be a generic property of many neurons since it can be obtained in biophysical compartmental models of conductance-based neurons, provided that synaptic noise is confined to a restricted window of values (Fig. 14B; [26]). Thus, it is likely that this observation can also explain the mapping of membrane potential to firing rate in a nearly exponential manner in the LGMD (Fig. 14C). It remains to be shown, however, whether the noise level lies in the appropriate range and whether the model generalizes to the higher firing rates observed experimentally in the LGMD neuron (compare Fig. 14A and B with 14C).

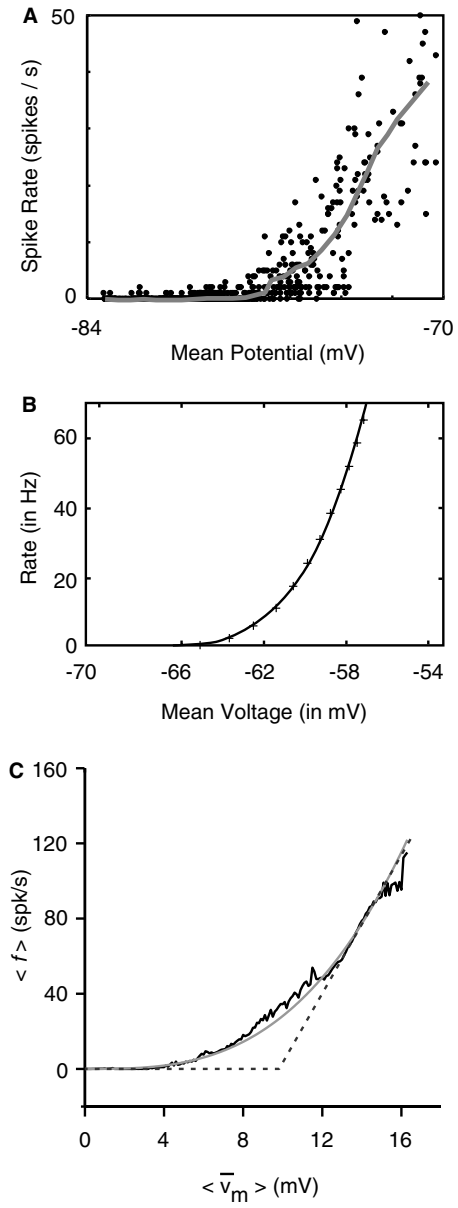

Fig. 14. Expansive non-linear relations between membrane voltage and firing rate in various preparations. (A) In visual cortical neurons of the cat, membrane potential and firing rate are related by a power law of exponent 2 (grey line). Adapted with permission from [4]. Copyright 2000 American Association for the Advancement of Science. (B) A single compartmental biophysical model with active membrane conductances yields a power law relation between membrane voltage and firing rate (exponent 3.5) in the presence of background noise. Adapted with permission from [26]. Copyright 2002 by the Society for Neuroscience. (C) Schematics illustrating how an approximate 3rd power law relation between membrane voltage and firing rate (fit in light grey, experimental data in black) could be obtained in the LGMD from a linear threshold model (dashed line) in the presence of noise. Adapted from [20].

8. Is multiplication a single cell or network computation?

Another question that arises is the role played by the presynaptic circuitry to the LGMD in the multiplicative computation described in the previous sections. The temporal dynamics underlying the activation of presynaptic afferents and their degree of synchronization during looming approach remains to be characterized. The results reported above demonstrate that two separate excitatory and inhibitory inputs are integrated within the LGMD and that exponentiation is approximately implemented at the level of its firing rate. It remains to be shown, however, where the early computational steps postulated by the model, such as the encoding of angular velocity in logarithmic coordinates, occur. Logarithmic compression of sensory inputs is a ubiquitous feature of sensory neuronal responses [37]. In the case of motion information it arise naturally in the context of the elementary motion detection model (EMD; Reichardt correlation model): the output of a multiplicative half- or full-correlation detector is known to a have logarithmic dependence on the velocity of a moving edge or sinusoidal grating pattern [89]. Thus, if the excitatory afferent input to the LGMD were processed according to this scheme, the logarithm of angular velocity would be taken presynaptically to the LGMD. An alternative possibility is for the logarithmic transformation to occur at the level of the synapse between excitatory LGMD afferent fibers and the cell, or entirely postsynaptically. This issue can in principle be addressed by characterizing the encoding of velocity

information at the level of presynaptic afferents to the LGMD as well as its postsynaptic transformation into LGMD membrane voltage. The role played by presynaptic versus postsynaptic elements in a multiplicative computation has recently been clarified in the encoding of directional motion information by rabbit retinal ganglion cells [16]. This computation is thought to rely on an inhibitory veto mechanism that is effectively observed to play an important role at the level of retinal ganglion cells [72]. Yet, recent evidence suggests that the distal dendritic compartments of starburst amacrine cells presynaptic to directionally selective ganglion cells already encode directionally selective information [16] and convey this information by a precise set of inhibitory synaptic connections to direction selective retinal ganglion cells [18]. This computation therefore relies on a multi-stage network processing of visual information.

9. Conclusions

Significant progress has recently been achieved in understanding the biophysics of neural multiplications in several different model systems [13,16,18,20,48]. It is not yet clear whether each of these computations relies on similar or different biophysical mechanisms, although some aspects of implementation may be conserved in different preparations (e.g., Section 7, Fig. 14). The visual system of insects proves to be particularly well suited for such investigations because it links up systems and cellular neurophysiology, allowing the application of a variety of techniques to tackle the issues related to the encoding and processing of information by individual identified neurons and small neuronal networks in vivo.

Acknowledgements

This work was supported by the Sloan Foundation, the National Institute of Mental Health (F.G., C.K.), the National Institute for Deafness and Communication Disorders (G.L.), the McKnight Foundation (G.L.) and the Center for Neuromorphic Engineering as part of the NSF Engineering Research Center programme. H.G.K. was supported by a travel grant of the Deutsche Forschungsgemeinschaft. F.G. is an Alfred P. Sloan research fellow.

References

[1] E. Adelson, J. Bergen, Spatiotemporal energy models for the perception of motion, J. Opt. Soc. Am. A 2 (1985) 284–299.
[2] R.A. Andersen, G.K. Essick, R.M. Siegel, Encoding of spatial location by posterior parietal neurons, Science 23 (1985) 456–458.
[3] J.C. Anderson, T. Binzegger, O. Kahana, K.A. Martin, I. Segev, Dendritic asymmetry cannot account for directional responses of neurons in visual cortex, Nat. Neurosci. 2 (1999) 820–824.
[4] J.S. Anderson, I. Lampl, D.C. Gillespie, D. Ferster, The contribution of noise to contrast invariance of orientation tuning in cat visual cortex, Science 290 (2000) 1968–1972.
[5] J.P. Bacon, K.S. Thompson, M. Stern, Identified octopaminergic neurons provide an arousal mechanism in the locust brain, J. Neurophysiol. 74 (1995) 2739–2743.
[6] H.B. Barlow, W.R. Levick, The mechanisms of directionally selective units in rabbit's retina, J. Physiol. (London) 178 (1965) 477–504.
[7] B. Bausenwein, A.P.M. Dittrich, K.-F. Fischbach, The optic lobe of *Drosophila melanogaster* II. Sorting of retinotopic pathways in the medulla, Cell Tiss. Res. 267 (1992) 17–28.
[8] A. Borst, J. Haag, Neural networks in the cockpit of the fly, J. Comp. Physiol. A 188 (2002) 419–437.
[9] M. Burrows, The neurobiology of an insect brain, Oxford University Press, Oxford, 1996.
[10] M. Burrows, C.H.F. Rowell, Connections between visual interneurons and methathoracic motorneurons in the locust, J. Comp. Physiol. 85 (1973) 221–234.
[11] M. Carandini, D. Ferster, Membrane potential and firing rate in cat primary visual cortex, J. Neurosci. 20 (2000) 470–484.
[12] P. Cavanagh, Size and position invariance in the visual system, Perception 7 (1978) 167–177.
[13] F.S. Chance, L.F. Abbott, A.D. Reyes, Gain modulation from background synaptic input, Neuron 35 (2002) 773–782.
[14] A. Borst, M. Egelhaaf, In vivo imaging of calcium accumulation in fly interneurons as elicited by visual motion stimulation, Proc. Natl. Acad. Sci. USA 89 (1992) 4139–4143.
[15] M. Elphick, L. Williams, M. O'Shea, New features of the locust optic lobe: evidence of a role for nitric oxide in insect vision, J. Exp. Biol. 199 (1996) 2395–2407.
[16] T. Euler, P.B. Detwiler, W. Denk, Directionally selective calcium signals in dendrites of starburst amacrine cells, Nature 418 (2002) 845–852.
[17] D. Ferster, K.D. Miller, Neural mechanisms of orientation selectivity in the visual cortex, Annu. Rev. Neurosci. 23 (2000) 441–471.
[18] S.I. Fried, T.A. Munch, F.S. Werblin, Mechanisms and circuitry underlying directional selectivity in the retina, Nature 420 (2002) 411–414.
[19] F. Gabbiani, H.G. Krapp, G. Laurent, Computation of object approach by a wide-field, motion-sensitive neuron, J. Neurosci. 19 (1999) 1122–1141.
[20] F. Gabbiani, H.G. Krapp, C. Koch, G. Laurent, Multiplicative computation in a looming-sensitive neuron, Nature 420 (2002) 320–324.
[21] F. Gabbiani, G. Laurent, N. Hatsopoulos, H.G. Krapp, The many ways of building collision-sensitive neurons, Trends Neurosci. 22 (1999) 437–438.
[22] F. Gabbiani, C. Mo, G. Laurent, Invariance of angular threshold computation in a wide-field looming-sensitive neuron, J. Neurosci. 21 (2001) 314–329.
[23] J.R. Gray, J.K. Lee, R.M. Robertson, Activity of descending contralateral movement detector neurons and collision avoidance behaviour in response to head-on visual stimuli in locusts, J. Comp. Physiol. 187 (2001) 115–129.
[24] M. Gewecke, K. Kirschfeld, R. Feiler, Identification of optic lobe neurons of locusts by video films, Biol. Cybern. 63 (1990) 411–420.
[25] J. Gouranton, Contribution à l'étude de la structure des ganglions cérébröides de *Locusta migratoria migratorioides*, Bull. Soc. Zool. France 89 (1964) 785–797.
[26] D. Hansel, C. van Vreeswijk, How noise contributes to contrast invariance of orientation tuning in cat visual cortex, J. Neurosci. 22 (2002) 5118–5128.

[27] B. Hassenstein, W. Reichardt, Systemtheoretische Analyse der Zeit-, Reihenfolgen- und Vorzeichenauswertung bei der Bewegungsperzeption des Ruesselkaefers Clorophanus, Z. Naturfor. 11 (1956) 513–524.
[28] N. Hatsopoulos, F. Gabbiani, G. Laurent, Elementary computation of object approach by a wide-field visual neuron, Science 270 (1995) 1000–1003.
[29] W.J. Heitler, Suppression of a locust visual interneurone (DCMD) during defensive kicking, J. Exp. Biol. 104 (1983) 203–215.
[30] G.R. Holt, C. Koch, Shunting inhibition does not have a divisive effect on firing rates, Neural Comput. 9 (1997) 1001–1013.
[31] G.A. Horridge, The separation of visual axes in apposition compound eyes, Philos. Trans. R. Soc. London B Biol. Sci. 285 (1978) 1–59.
[32] F. Killmann, H. Gras, F.-W. Schuermann, Types, numbers and distribution of synapses on the dendritic tree of an identified visual interneuron in the brain of the locust, Cell Tissue Res. 296 (1999) 645–665.
[33] C. Koch, T. Poggio, V. Torre, Nonlinear interactions in a dendritic tree: localization, timing, and role in information processing, Proc. Natl. Acad. Sci. USA 80 (1983) 2799–2802.
[34] C. Koch, Biophysics of computation: Information processing in single neurons, Oxford University Press, Oxford, 1998.
[35] H.G. Krapp, R.A. Hengstenberg, A fast stimulus procedure to determine local receptive field properties of motion-sensitive visual interneurons, Vision Res. 37 (1997) 225–234.
[36] R. Kurtz, V. Duerr, M. Egelhaaf, Dendritic calcium accumulation associated with direction-selective adaptation in visual motion-sensitive neurons in vivo, J. Neurophysiol. 84 (2000) 1914–1923.
[37] S.B. Laughlin, Form and function in retinal processing, Trends Neurosci. 10 (1987) 478–483.
[38] S.B. Laughlin, R.C. Hardie, Common strategies for light adaptation in the peripheral visual systems of fly and dragonfly, J. Comp. Physiol. 128 (1978) 319–340.
[39] M.S. Livingstone, Mechanisms of direction selectivity in macaque V1, Neuron 20 (1998) 509–526.
[40] C.J. McAdams, J.H.R. Maunsell, Effects of attention on orientation-tuning functions of single neurons in macaque cortical area V4, J. Neurosci. 19 (1999) 431–441.
[41] C. Mead, Analog VLSI and Neural Systems, Addison-Wesley, Boston, MA, 1989.
[42] C.I. Miles, Temperature compensation in the nervous system of the grasshopper, Physiol. Entomol. 17 (1992) 169–175.
[43] K.D. Miller, T.W. Troyer, Neural noise can explain expansive, power-law nonlinearities in neural response functions, J. Neurophysiol. 87 (2002) 653–659.
[44] M. O'Shea, C.H.F. Rowell, J.L.D. Williams, The anatomy of a locust visual interneurone; the descending contralateral movement detector, J. Exp. Biol. 60 (1974) 1–12.
[45] M. O'Shea, C.H.F. Rowell, Protection from habituation by lateral inhibition, Nature 254 (1975) 53–55.
[46] M. O'Shea, C.H.F. Rowell, The neuronal basis of a sensory analyzer, the acridid movement detector system II. Response decrement, convergence, and the nature of the excitatory afferents to the fan-like dendrites of the LGMD, J. Exp. Biol. 65 (1976) 289–308.
[47] M. O'Shea, J.L.D. Williams, The anatomy and output connection of a locust visual interneurone; the lobula giant movement detector (LGMD) neurone, J. Comp. Physiol. 91 (1974) 257–266.
[48] J.L. Pena, M. Konishi, Auditory spatial receptive fields created by multiplication, Science 292 (2001) 249–252.
[49] K.G. Pearson, C.S. Goodman, Correlation of variability in structure with variability in synaptic connections of an identified interneuron in locusts, J. Comp. Neurol. 184 (1979) 141–166.
[50] K.G. Pearson, W.J. Heitler, J.D. Steeves, Triggering locust jump by multimodal inhibitory interneurons, J. Neurophysiol. 43 (1980) 257–278.
[51] R.B. Pinter, R.M. Olberg, T.W. Abrams, Is the locust DCMD a looming detector? J. Exp. Biol. 101 (1982) 327–331.
[52] J.J. Rauh, S.C.R. Lummis, D.B. Sattelle, Pharmacological and biochemical properties of insect GABA receptors, Trends Pharmacol. 11 (1990) 325–329.
[53] F.C. Rind, E.W. Childs, Collision avoidance in locusts: the role of attention in modulating performance, in: Proceedings of the International Conference on Invertebrate Vision, Baeckaskog Castle, Sweden, 2001.
[54] F.C. Rind, Intracellular characterization of neurons in the locust brain signaling impending collision, J. Neurophysiol. 75 (1996) 986–995.
[55] F.C. Rind, D.I. Bramwell, Neural network based on the input organization of an identified neuron signaling impending collision, J. Neurophysiol. 75 (1996) 967–985.
[56] F.C. Rind, G. Leitinger, Immunocytochemical evidence that collision sensing neurons in the locust visual system contain acetylcholine, J. Comp. Neurol. 423 (2000) 389–401.
[57] F.C. Rind, P.J. Simmons, Orthopteran DCMD neuron: a reevaluation of responses to moving objects.I. Selective responses to approaching objects, J. Neurophysiol. 68 (1992) 1654–1666.
[59] F.C. Rind, P.J. Simmons, Local circuits for the computation of object approach by an identified visual neuron in the locust, J. Comp. Neurol. 395 (1998) 405–415.
[60] R.M. Robertson, A.G. Johnson, Retinal image size triggers obstacle avoidance in flying locusts, Naturwissenschaften 80 (1993) 176–178.
[61] R.M. Robertson, D.N. Reye, Wing movements associated with collision-avoidance manoeuvres during flight in the locust Locusta migratoria, J. Exp. Biol. 163 (1992) 231–258.
[62] E.T. Rolls, G.C. Baylis, Size and contrast have only small effects on the responses to faces of neurons in the cortex of the superior temporal sulcus of the monkey, Exp. Brain Res. 65 (1986) 38–48.
[63] C.H.F. Rowell, Variable responsiveness of a visual interneurone in the free-moving locust, and its relation to behavior and arousal, J. Exp. Biol. 55 (1971) 727–747.
[64] C.H.F. Rowell, The orthopteran descending movement detector (DMD) neurons: a characterization and review, Z. vergl. Physiol. 73 (1971) 167–194.
[65] C.H.F. Rowell, Boredom and attention in a cell in the locust visual system, in: L.B. Browne (Ed.), Experimental Analysis of Insect Behavior, Springer-Verlag, New York, 1974, pp. 87–99.
[66] C.H.F. Rowell, M. O'Shea, The neuronal basis of a sensory analyzer, the acridid movement detector system I. Effects of simple incremental and decremental stimuli in light and dark adapted animals, J. Exp. Biol. 65 (1976) 273–288.
[67] C.H.F. Rowell, M. O'Shea, J.L.D. Williams, The neuronal basis of a sensory analyzer, the acridid movement detector system IV. The preference for small field stimuli, J. Exp. Biol. 68 (1977) 157–185.
[68] R.A. Satterlie, Structural variability of an identified interneurone in locusts from a wild population, J. Exp. Biol. 114 (1985) 691–695.
[69] G. Sary, R. Vogels, G.A. Orban, Cue-invariant shape selectivity of macaque inferior temporal neurons, Science 260 (1993) 995–997.
[70] G.R. Schlotterer, Response of the locust descending movement detector neuron to rapidly approaching and withdrawing visual stimuli, Can. J. Zool. 55 (1977) 1372–1376.
[71] E.L. Schwartz, R. Desimone, T.D. Albright, C.G. Gross, Shape recognition and inferior temporal neurons, Proc. Natl. Acad. Sci. USA 80 (1983) 5776–5778.
[72] S.F. Stasheff, R.H. Masland, Functional inhibition in direction-selective retinal ganglion cells: spatiotemporal extent and intralaminar interactions, J. Neurophysiol. 88 (2002) 1026–1039.

[73] M. Stern, M. Gewecke, Spatial sensitivity profiles of motion sensitive neurons in the locust brain, in: K. Wiese et al. (Eds.), Sensory Systems of Arthropods, Birkhaeuser Verlag, Basel, 1993, pp. 184–195.
[74] N.J. Strausfeld, A.D. Blest, The optic lobes of Lepidoptera, Philos. Trans. R. Soc. London 258 (1971) 81–134.
[75] N.J. Strausfeld, Functional neuroanatomy of the blowfly's visual system, in: M.A. Ali (Ed.), Photoreception and Vision in Invertebrates, Plenum Press, New York, 1984, pp. 483–522.
[76] N.J. Strausfeld, J.-K. Lee, Neuronal basis for parallel visual processing in the fly, Vis. Neurosci. 7 (1991) 13–33.
[77] N.J. Strausfeld, D.R. Naessel, Neuroarchitecture serving compound eyes of crustacea and insects, in: H. Autrum (Ed.), Comparative Physiology and Evolution of Vision of invertebrates. B: Invertebrate Visual Centers and Behavior I. Handbook of Sensory Physiology, vol. VII/6B, Springer-Verlag, Berlin, 1981, pp. 1–132.
[78] G. Stuart, N. Spruston, M. Hausser, Dendrites, Oxford University Press, Oxford, 1999.
[79] H. Sun, B.J. Frost, Computation of different optical variables of looming objects in pigeon nucleus rotundus neurons, Nat. Neurosci. 1 (1998) 296–303.
[80] V. Torre, T. Poggio, A synaptic mechanism possibly underlying directional selectivity to motion, Proc. R. Soc. London B 202 (1978) 409–416.
[81] S. Treue, J.H. Maunsell, Effects of attention on the processing of motion in macaque middle temporal and medial superior temporal visual cortical areas, J. Neurosci. 19 (1999) 7591–7602.
[82] B.A. Trimmer, Current excitement from insect muscarinic receptors, Trends Neurosci. 18 (1995) 104–111.
[84] W.-T. Fogh, Biology and physics of locust flight VIII. Lift and metabolic rate of flying locusts, J. Exp. Biol. 41 (1964) 257–271.
[86] A.K. Warzecha, M. Egelhaaf, A. Borst, Neural circuit tuning fly visual interneurons to motion of small objects. 1. Dissection of the circuit by pharmacological and photoinactivation techniques, J. Neurophysiol. 69 (1993) 329–339.
[87] H. Xu, R.M. Robertson, Neural parameters contributing to temperature compensation in the flight CPG of the locust, *Locusta migratoria*, Brain Res. 734 (1996) 213–222.
[89] J.M. Zanker, M.V. Srinivasan, M. Egelhaaf, Speed tuning in elementary motion detectors of the correlation type, Biol. Cybern. 80 (1999) 109–116.
[90] M. Zaretsky, C.H.F. Rowell, Saccadic suppression by corollary discharge in the locust, Nature 280 (1979) 583–584.